International Conference on Space Optics—ICSO 2018

Chania, Greece

9–12 October 2018

Edited by Zoran Sodnik, Nikos Karafolas, and Bruno Cugny

Protected silver coatings for reflectors

Stefan Schwinde

Mark Schürmann

Ralph Schlegel

Jan Kinast

et al.

International Conference on Space Optics — ICSO 2018, edited by Zoran Sodnik, Nikos Karafolas, Bruno Cugny, Proc. of SPIE Vol. 11180, 111804M · © 2018 ESA and CNES · CCC code: 0277-786X/18/$18 · doi: 10.1117/12.2536085

Protected silver coatings for reflectors

Stefan Schwinde*[a], Mark Schürmann[a], Ralph Schlegel[a], Jan Kinast[a], Reinhold J. Dorn[b], Jean Louis Lizon[b], Sebastien Tordo[b], Norbert Kaiser[a]
[a]Fraunhofer Institute for Applied Optics and Precision Engineering IOF, Albert-Einstein-Strasse 7, D-07745 Jena, Germany; [b]European Southern Observatory ESO
Karl-Schwarzschild-Straße 2, D-85748 Garching bei Muenchen, Germany

*stefan.schwinde@iof.fraunhofer.de

ABSTRACT

For ground- and spaced based applications, Ag coated reflectors are indispensable because of their high reflectivity. The transport, assembling and storage of these reflectors takes a long time, before they are finally commissioned for the actual applications. To endure this period without a decrease of reflectivity, protective coatings with a final layer, which offers a high resistance to aqueous solutions and a low mechanical stress should be used. These criteria were taken into account for the selection of a final layer for a protected Ag-coating, which was applied for reflectors utilized in the CRIRES$^+$-instrument (an IR spectrograph used at the VLT). Reactively sputtered Al_2O_3, SiO_2 and Si_3N_4 layers were investigated with regard to these criteria. In aqueous (basic) solutions, the investigated Si_3N_4 layers are more stable than the SiO_2 layers, and the SiO_2 layers are more stable than the Al_2O_3 layers. This shows the influence of the intrinsic material properties. The mechanical stress of the sputtered layers depends on the deposition conditions and thus on the selected parameters. A Si_3N_4 layer with a high resistance to aqueous solutions also offers a low and stable mechanical stress. Therefore, the deposition-parameters which have been used for this layer were applied for sputtering the final layer of the protected Ag-coating for the reflectors.

Keywords: Protective layer, coating, sputtering, silver, reflector, durability.

1. INTRODUCTION

Metals have a high reflectivity in a broad spectral range [1]. Of all metals, Ag has the highest reflectivity in the visible spectral range (VIS) and the short wavelength part of the IR range. Therefore, Ag coatings are indispensable for highly reflective components such as reflectors [1]. Under ambient conditions, the high reflectivity of unprotected Ag coatings unfortunately decreases rapidly due to the formation of compounds like Ag_2S, AgCl or Ag_2O [2–6]. To avoid a rapid decrease of reflectivity Ag coatings with one or more sealing protection layers (protected Ag) are applied for reflectors. But even in the case of protected Ag, the appearance of defects which could decrease the reflectivity has to be considered [7–11]. This consideration and moreover the improvement of mirror durability due to the protection of Ag is an ongoing research topic [11]. This article is a contribution to the improvement of protected silver coatings for reflectors.

For a coated reflector, the requirements concerning its durability differ strongly depending on the relevant environmental conditions for the application (e.g. between ground- and spaced based reflectors, or primary mirrors and reflectors located inside of a device). Leaving the different applications aside, the time span between the deposition of the highly reflecting coating and the actual application often exceeds months and sometimes years. In this period, transport, assembling and storage in several laboratories expose the coated reflectors to different environmental conditions [8, 12]. Therefore, reflectors for ground- and spaced-based applications have to be durable under these conditions. During the transport, assembling and storage, conditions like temperature, humidity and air pollution are only controllable with great effort. The existence of high humidity can lead to condensation on the reflectors surface. Due to hygroscopic airborne particles condensation on the coated reflector is also possible at a relative humidity of < 80 % [13]. Beside the unintended condensation, a cleaning process of the coated mirror can require a sufficient resistance to liquid solutions.

Regarding the resistance of the coated reflectors to liquid solutions, a distinction between acidic and basic solutions is practicable. The material Si_3N_4 can offer a high resistance against acid [14] but shows significant reactions in a basic solution [15]. SiO_2 also has a high resistance to most of the acids. If SiO_2 is exposed to a basic solution, a higher

concentration of OH-ions goes along with a stronger reaction of SiO_2 [16, 17]. The material Al_2O_3 also reacts with basic solutions [13]. Therefore, when these materials are used to protect an Ag-layer, the durability to basic solution is of special interest. Because of this, investigations with an aqueous base were executed to determine a protective layer which is stable, even in a basic solution, and thus can contribute to an improved durability of the protected Ag-coating.

In addition to a high resistance to liquid solutions, the protective layer of an Ag coating should have a low mechanical stress. Tensile stresses can lead to cracks in the protective layer, and compressive stresses can lead to delamination of the protective layer [18–20]. Both, cracks or delamination, lead to a damage of the protected Ag-coating and result in a decrease of specular reflectivity.

Reactive sputtering is a suitable method for the deposition of Ag, Al_2O_3, SiO_2 and Si_3N_4. With regards to the mentioned criteria for protective layers (high resistance to aqueous bases and a low mechanical stress) the materials Al_2O_3, SiO_2 and Si_3N_4 have been investigated. The intrinsic material properties as well as the deposition-related layer-properties have been taken into account. For the generic consideration of the influence of deposition conditions, process curves were used for the sputtering of the oxides [21]. SiN_x was already successfully applied as a final layer of a protected Ag-coating for the Gemini Telescopes [9] and the Kepler-Space Telescope [22]. Therefore, a detailed and comparative investigation of the potential of Si_3N_4, with regards to the critical properties of high resistance against aqueous solutions and a low mechanicals stress was undertaken.

The findings of the above mentioned research have been used to determine a final layer for a protected Ag-coating, which was applied for reflectors utilized in the CRIRES$^+$-instrument. The reflectors were manufactured (by diamond turning and polishing) and coated at the Fraunhofer IOF in Jena [23]. The CRIRES$^+$-instrument is an instrument which will be installed at the Very Large Telescope (VLT). It is an infrared (0.92–5.2 μm) high-resolution cross-dispersed spectrograph which enables astrophysical activities like search for exoplanets and cosmology [24]. In the period after the coating and before the application, the environmental conditions of these reflectors are comparable to the conditions existing for other high-tech reflectors. Also for space based reflectors, a long period of transport, assembling and storage before launch and application have to be taken into account. Thus, for all these Ag-coated reflectors, a protective layer with a final layer which offers a high resistance to aqueous solutions and a low mechanical stress should be applied.

2. METHOD

2.1 Process curves and sample deposition

The generation of process curves and the layer deposition was carried out in an inline sputtering system with a top-down arrangement. The target geometry of this system is 750 mm × 100 mm. During the process, the substrate scans vertical to the narrow side of the target. The layer thickness is controlled by determining the deposition rate in a preliminary test and adjusting the number of scans and scan-velocity. Al_2O_3, SiO_2 and Si_3N_4 were sputtered by reactive dual-magnetron sputtering with MF-voltage from an Al- or a Si-target, respectively. The sputtering of these three materials was done with a power of 4 kW. Ag was sputtered from an Ag target by DC-sputtering with a power of 5 kW. The background pressure was below 3×10^{-6} mbar. Ar was used as working gas and O_2 or N_2 were used as reactive gases. During the layer-deposition, Ar and N_2 were delivered into the coating chamber with a constant flow, while the oxygen partial pressure in the chamber was controlled by a feedback control system. The actual value of the oxygen partial pressure was not measured directly. With a ZIROX XS22.3H vacuum probe a lambda probe value “L” was determined. This value is directly inverse in proportion to the oxygen partial pressure in the coating chamber. The pumping power of the inline sputtering system was kept constant during the experiments.

In the case of oxides (Al_2O_3, SiO_2), S-shaped process curves have been generated by using the oxygen partial pressure as the control parameter. The lambda probe value L varied while the supply of the associated oxygen (gas flow into the coating-chamber) was recorded. The theoretical background of this kind of process curves is described in detail in the literature [21, 25, 26]. Three different values of Ar supply (gas flow into the chamber: 20 sccm, 90 sccm or 160 sccm) were used, whereby three different process curves could be generated. These curves are shown in figure 1. For each Ar-supply and thus for each process curve, an operation area has been determined (see figure 1). The sample deposition was done for every determined operation area. Thus, Al_2O_3 and SiO_2 where deposited under three different conditions each.

Si_3N_4 has been deposited with four different sets of coating parameters. The deposition of the sample was done with an Ar-supply of 20 sccm in combination with a low supply of N_2 (33 sccm) and a high supply of N_2 (120 sccm). In addition,

the sample deposition was done with an Ar supply of 80 sccm in combination with a low supply of N_2 (47 sccm) and a high supply of N_2 (120 sccm).

In each deposition run (3 x Al_2O_3, 3 x SiO_2, 4 x Si_3N_4), a 3-inch Si-wafer and a smaller Si-substrate were placed, for the investigation of the film stress and the solubility behavior respectively. The layer thickness of the prepared samples is in the range of 280 nm ± 40 nm. The investigated samples and the dynamic deposition rates from the sample deposition are summarized in table 1.

2.2 Solubility behavior of reactive sputtered layers

To determine the properties of the reactive sputtered layers (Al_2O_3, SiO_2 and Si_3N_4) regarding their solubility, these layers were deposited on polished Si-substrates. These samples were exposed to a solution, which consisted of distilled water with a certain amount of Na_2S. The exposure was interrupted frequently to determine the remaining layer thickness of the layers. With the help of this approach, it was possible to determine the removal rate of the layers in aqueous solution.

In a first test, all samples were exposed to a solution which consist of distilled water and 0.13 m% Na_2S. This solution has a pH-value between 11 and 11.5. The frequent determination of layer thickness was carried out by IR absorption spectroscopy with a Varian 3100 FTIR. The characteristic peaks resulting from absorption due to Al_2O_3, SiO_2 or Si_3N_4 have been analyzed. In this first test, only the Al_2O_3 layers and the layer "SiO_2_160Ar" reveal a significant decrease of layer thickness. This decrease is shown in Figure 2. The negative slope represents the removal rate. The slope and the uncertainty of the measurement were determined by linear regression.

Those samples which show no significant decrease in the first test were exposed to a solution consisting of distilled water and 0.63 m% Na_2S. This solution has a pH-value between 12,5 and 13. The determination of the remaining layer thickness was not based on absorption spectroscopy, like in the first test, but on optical characterization. For this determination, the measurement of reflectivity in a spectral range from 400 nm to 1100 nm by a spectrophotometer (Lambda 850/900/950 from Perkin Elmer) and a subsequent characterization of the measurement by the software OptiChar [27] was realized (a dispersion model according to the Cauchy equation was applied). The reason for the change of the determination of the layer thicknesses is a lower measurement uncertainty for the optical characterization. The results of this second test are shown in Figure 3. The negative slope represents the removal rate. The slope and the uncertainty of the measurement were determined by linear regression.

2.3 Mechanical stress in reactive sputtered layers

A Tencor FLX-2320 was used to determine the deflections of polished Si-wafers (3 ") before and after the coating. Taking the layer geometry, the wafer geometry, the intrinsic material properties of the substrate and the change of deflection into account, the stress of the coated layers can be determined by applying the Stoney equation [28]. With this method, the stress of the coated layers was determined frequently (over a period > 3500 h after coating). The repeatability of measurements was < 5 MPA and the measurement uncertainty for the absolute value is <30 MPa. During the period of frequent measurements, the samples were stored under ambient conditions of 45% ± 20% humidity and a temperature of 23 ° C ± 4 ° C. The determined stress is compressive, which is indicated by the minus sign.

3. RESULTS

3.1 Process curves and sample deposition for reactive sputtering

For Al_2O_3 and SiO_2, the S-shaped process curves for reactive sputtering with O_2 could be generated by using the partial pressure of oxygen as a control parameter (figure 1). As described in the literature [21, 25, 26], these curves reveal areas, where sputtering takes place in the metallic mode, in the transition mode and in the compound mode:

Sputtering in the metallic mode takes place if the operating point is in the part of the process curve that stresses from the lowest oxygen partial pressure to the first inflection point. In this mode, the target is predominantly not poisoned due to reactions with a reactive gas. Thus, mainly the pure target material is sputtered. Sputtering in this mode often results in a deposition of layers which are highly absorbing in the visual spectral range. Therefore, this mode is not suitable for the deposition of protective layers for Ag-coatings.

Sputtering in the transition mode takes place if the operating point is between the first and the second inflection point. In this mode, the surface of the target is partly occupied by the reaction products (Al_2O_3 or SiO_2).

Sputtering in the compound mode takes place, if the operating point is in the part of the process curve that stresses from the second inflection point in the direction of higher oxygen partial pressure. In this mode, the surface of the target is predominantly poisoned with Al_2O_3 or SiO_2 respectively. The deposition rate for sputtering in the compound mode is expected to be lower than for sputtering in the transition mode and in the metallic mode.

Like shown in figure 1 and table 1, the sample deposition has been done with operating points in the transition mode. Thereby the sputtering of transparent layers with a relatively high deposition rate (compared to the sputtering in the compound mode) was carried out. The only exception is the SiO_2 layer which was sputtered with an Ar supply of 20 sccm and an operating point in the compound mode. The deposited rate of this SiO_2 layer is lower than the deposition rate of the other SiO_2 layers (table 1).

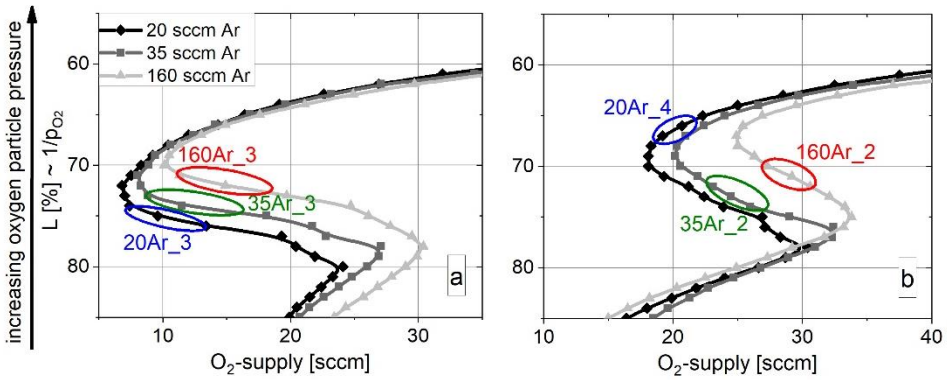

Figure 1: S-shaped process curves for the reactive sputtering of Al_2O_3 (a) and SiO_2 (b). The curves differ with respect to the supply of working gas (Ar). The areas show the location of the operating points for the different Ar-supplies.

The chosen parameters for the Si_3N_4 have an influence on the deposition rate. A higher supply of N_2 leads to a lower deposition rate. This is true for a supply of working gas (Ar) of 20 sccm and of 80 sccm (table 1).

Table 1. Investigated layers (deposited on substrates), their sputtering conditions and the resulting deposition rate.

Layer	Ar-flow [sccm]	operating point	N_2-supply [sccm]	Dynamic deposition rate [nm*m/min]
Al_2O_3_20Ar	20	transition mode		3
Al_2O_3_35Ar	35	transition mode		3
Al_2O_3_160Ar	160	transition mode		3
SiO_2_20Ar	20	compound mode		8
SiO_2_35Ar	35	transition mode		17
SiO_2_160Ar	160	transition mode		19
Si_3N_4_1	20		33	12
Si_3N_4_2	20		120	7
Si_3N_4_3	80		47	12
Si_3N_4_4	80		120	8

3.2 Solubility behavior of reactively sputtered layers

The exposure of the samples to an aqueous (basic) solution reveals that the removal rates of the three different Al_2O_3 layers are higher than the removal rates of all other tested layers (three different SiO_2 layer and 4 different Si_3N_4 layer). Even in an aqueous solution with a relative low pH-value between 11.0 and 11.5, these layers dissolve within a few hours (Figure 2 a). Furthermore, the SiO_2 layer “SiO2_160Ar" shows a removal rate in the aqueous solution with a pH-value between

11.0 and 11.5 (Figure 2 b), even though this removal rate is significantly lower than the one of the Al_2O_3 layers. The SiO_2 layers sputtered with a lower supply of Ar and the Si_3N_4 do not show a significant decrease in layer thicknesses due to exposure to the aqueous solution with a pH-value between 11.0 and 11.5.

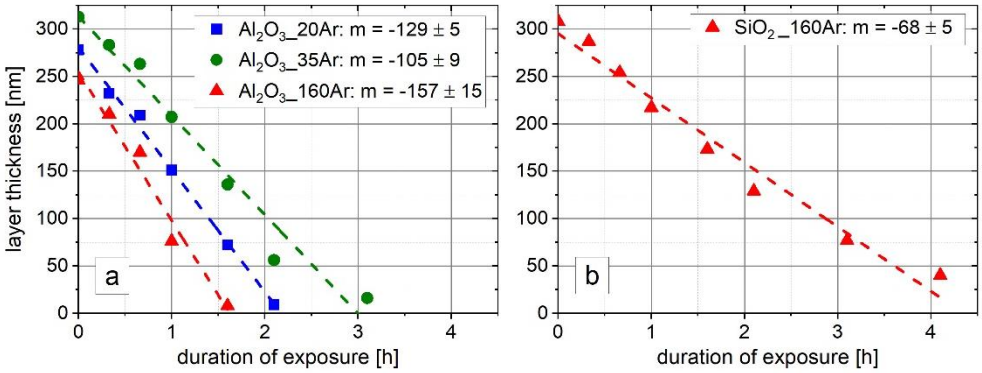

Figure 2: Removal rates in nm / h of the Al2O3 layers (a) and the SiO2 layer "160Ar_2" in a basic solution (pH-value between 11 and 11.5), expressed through the negative slope m.

Figure 3 shows the decrease of layer thickness for an aqueous solution (pH-value between 12.5 and 13). The SiO_2-layer sputtered with an Ar supply of 35 sccm in the transition mode is less stable than the SiO_2 sputtered with an Ar supply of 20 sccm in the compound mode. However, the least stable layer of SiO_2 is still more stable than the best Al_2O_3-layer. Furthermore, the least stable of the Si_3N_4 layers (Si3N4_3) is still more stable than the best SiO_2-layer (SiO_2_20Ar).

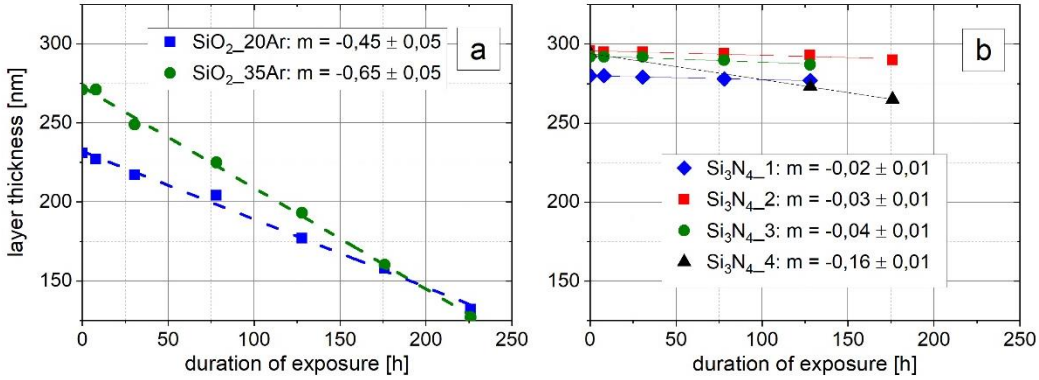

Figure 3: Removal rate in nm / h of the SiO2 layers "SiO2_20Ar" and "SiO2_35Ar" (a) and the Si3N4 layers (b) in a basic solution (pH-value between 12.5 and 13), expressed through the negative slope m.

3.3 Mechanical stress in reactive sputtered layers

The layer stress (compressive stress) of the three investigated Al_2O_3 layers is between -145 MPa and -210 MPa (Figure 3 a). The layers did not show a significant change of layer stress (above 10 MPa) in a time period of more than 3500 h.

The SiO_2 layers show a significant change of layer stress (figure 3 b). The layer "SiO_2_35Ar" shows a crucial increase of compressive stress of more than 120 MPa. The sample "SiO_2_160Ar" shows a variation of the compressive stress of ~ 40 MPa and thus also a significant change of layer stress. The sample "SiO_2_20Ar" has the most stable SiO_2-layer. However, a small increase in the compressive stress of ~ 10 MPa over a period of > 3500 h should be considered.

The Si_3N_4 layers show huge differences with regard to the mechanical stress. The Si_3N_4 layers sputtered with an Ar supply of 20 sccm have a high compressive stress of approximately -1490 MPa (Si_3N_4_1) and approximately -670 MPa (Si_3N_4_2). In contrast, the Si_3N_4 layers sputtered with an Ar supply of 80 sccm (Si_3N_4_3 and Si_3N_4_4) have a low compressive stress between -20 and -90 MPa. In case of the Si_3N_4, the layer Si_3N_4_4 shows a significant change of layer stress (figure 4 c and d).

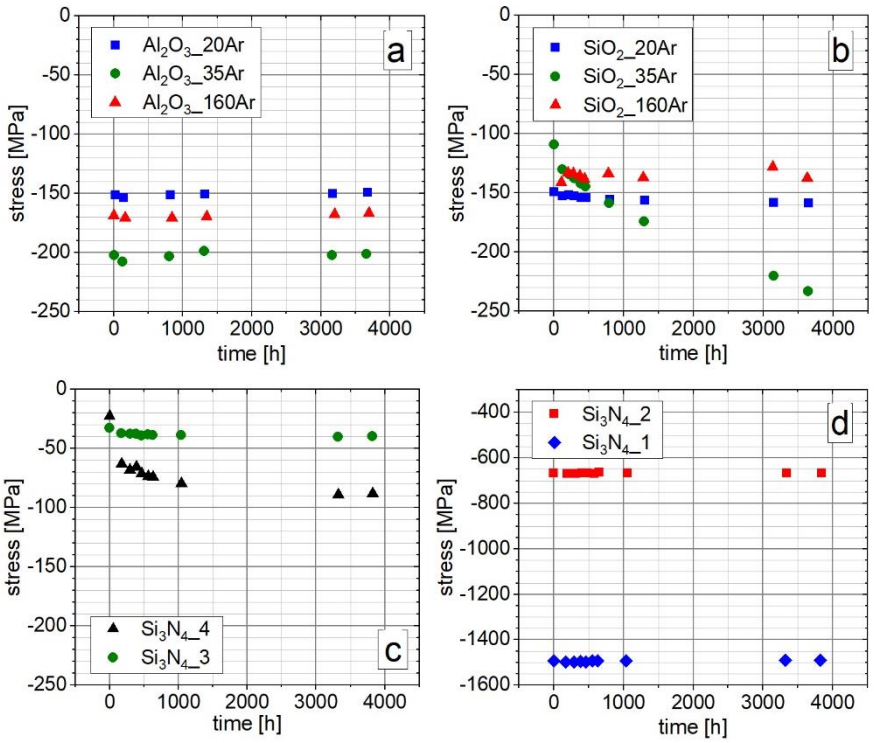

Figure 4: Progress of the compressive stresses of sputtered Al_2O_3 (a), SiO_2 (b), and Si_3N_4 (c and d).

4. DISCUSSION

4.1 Process curves and sample deposition

S-shaped process curves for reactive sputtering can be generated as described in the literature [21, 25, 26], whereby an interpretation of the influence of the sputter parameter is possible. The lower deposition rate for oxides (SiO_2), sputtered with an operating point in the compound mode instead of in the transition mode stands in accordance with the literature [29]. The reason for this behavior is that the sputter yield of the compound material (e.g. SiO_2) is often lower than the sputter yield of the pure (target-) material (e.g. Si) [26]. A lower sputter yield for the compound material as for the pure (target-) material could also explain why Si_3N_4 sputtered with a higher supply of N_2 has a lower deposition rate than Si_3N_4 sputtered with a low supply of N_2.

4.2 Solubility behavior of reactive sputtered layers

With regard to the solubility behavior of the sputtered layers, an influence of the intrinsic material properties and of the deposition parameters are visible.

Since the most stable Al_2O_3 layer (lowest removal rate) is less stable than the most unstable SiO_2 layer, and the most stable SiO_2 layer is less stable than the most unstable Si_3N_4 layer, the influence of the intrinsic material properties is evident. These significant differences can be explained by the different bonds of the materials. Due to the application of "Fanjans rules", it can be estimated that the fraction of covalent bonds increases from Al_2O_3 to SiO_2 to Si_3N_4. These rules consider how far the cation polarizes the anion and thereby increases the fraction of covalent bonds which leads to a higher resistance in polar solutions [30]. A small radius (r_{cation}) and a high charge (z_{cation}) of cations, as well as a large radius (r_{anion}) and high charges (z_{anion}) of anions lead to an increase of the covalent fraction. To estimate and compare the potential of the building of covalent bonds, calculations are possible [30, 31]. The potential of the building of covalent bonds has been calculated for the three tested materials (Al_2O_3, SiO_2 and Si_3N_4) with the following equation:

$$\text{potential for covalent bonds } [e^2] = \frac{z_{cation}\, r_{anion}\, z_{anion}}{r_{cation}}$$

Assuming the charges and ionic radii given in table 2, the potential for the building of covalent bonds is as follows: Al_2O_3 = 13, SiO_2 = 21 and Si_3N_4 = 34. Thus, the influence of the intrinsic material properties with regards to solubility behavior can be explained.

Table 2: Binding partner and corresponding ionic radius [30].

	cations		**anions**	
binding partner	Al^{3+}	Si^{4+}	O^{2-}	N^{3-}
ionic radii [nm]	0,060	0,047	0,125	0,132

In addition to the intrinsic material properties the deposition parameters have a significant influence on the solubility behaviour of the investigated layers. For Al_2O_3 and for SiO_2, the most unstable layer is the one sputtered with the highest supply of Ar (160 sccm). Since the pumping of the coating-chambers was done with a constant rate in all deposition runs, a higher supply of Ar leads to a higher pressure in the chamber. The higher pressure leads to a higher probability of inelastic scattering between Ar and sputtered adatoms, whereby the kinetic energy of the adatoms is reduced. A reduced kinetic energy of the adatoms can lead to an porose layer structure with an higher specific surface [32-34], whereby a higher removal rate of layer-thickness in an aqueous solution can be explained.

4.3 Mechanical stress in reactive sputtered layers

In contrast to these Al_2O_3 layers, the SiO_2 layers show a significant change of mechanical stress due to storage at ambient conditions. The change of stress can result from an interaction between water from the environment and the SiO_2-layers. The penetration of water into a layer can lead to water-induced stresses [19] which can be tensile stresses [35] or compressive stresses [19, 36]. For (vapor-deposited) SiO_2 layers in particular, the occurrence of water-induced stresses has been published [19, 36–39]. Water-induced stress could also be the reason for the unstable stress of the layer Si3N4_4.

The high compressive stress for sputtered Si_3N_4 layers (circa -1,5 GPa) is in accordance with results found in the literature [40]. In both cases, our findings and the findings descripted in the literature, the high compressive stress results from sputtering with a low working pressure or with a low Ar-supply, respectively [40]. Like discussed above, a higher working pressure leads to a higher probability of inelastic scattering between Ar and sputtered adatoms, whereby the kinetic energy of the adatoms is reduced and the microstructure of the layer becomes more porous [32-34]. A more porous microstructure can lead to lower compressive stress or higher tensile stress. The correlation between a low working pressure during sputtering and a compact and dense microstructure, which often goes together with compressive stress, is already described for Si_3N_4 [41]. Thus, the low stress for the Si_3N_4 layers sputtered with an Ar-supply of 80 sccm (Si_3N_4_3 and Si_3N_4_4) can be explained.

5. CONCLUSION

For ground- and spaced based applications, Ag coated reflectors are indispensable because of the high reflectivity of Ag. A long period of transport, assembling and storage of these reflectors take place, before they are used for the actual applications. To endure this period without a decrease of reflectivity, protective layers with a final layer which offers a high resistance to aqueous solutions and a low mechanical stress should be used.

Typical protective layers like Al_2O_3 and SiO_2 can be deposited by reactive sputtering. S-shaped process curves for reactive sputtering with O_2 are useful for the interpretation of the deposition conditions and an optimization of the layer properties. E.g., sputtering SiO_2 with a more poisoned target results in a lower deposition rate but can increase the resistance of the sputtered layer to aqueous solutions.

With regards to the resistance of the investigated Al_2O_3, SiO_2 and Si_3N_4 to aqueous solutions, the influence of the intrinsic material properties is higher than the influence of the deposition conditions. All Si_3N_4 layers are more stable than SiO_2, and all SiO_2 layers are more stable than Al_2O_3. Although the sputtered Si_3N_4-layers offer by far the best sustainability in aqueous (basic) solutions, not all of these layers are suitable as a final layer of the protective coating for Ag. In two cases

(Si_3N_4_1 and Si_3N_4_2) the compressive stress is too high, because it harbors the danger of delamination. In case of Si_3N_4_4, the stress is shifted and thus the layer is not stable. Fortunately, the layer Si_3N_4_3 fulfilled both conditions, a high resistance to aqueous solutions and a low mechanical stress. Therefore, the parameters which have been used for the deposition of the layer Si_3N_4_3 were also used for the deposition of the final layer for the protected Ag-coating, which was applied for reflectors utilized in the CRIRES$^+$-instrument (used at VLT). This protective coating, with the Si_3N_4 layer of high durability and low mechanical stress as a final layer, was designed and fabricated following a patented approach [42]. The optical performance for the protected Ag-coating for the CRIRES$^+$-instrument (a spectrograph for the IR-range) is shown in figure 5.

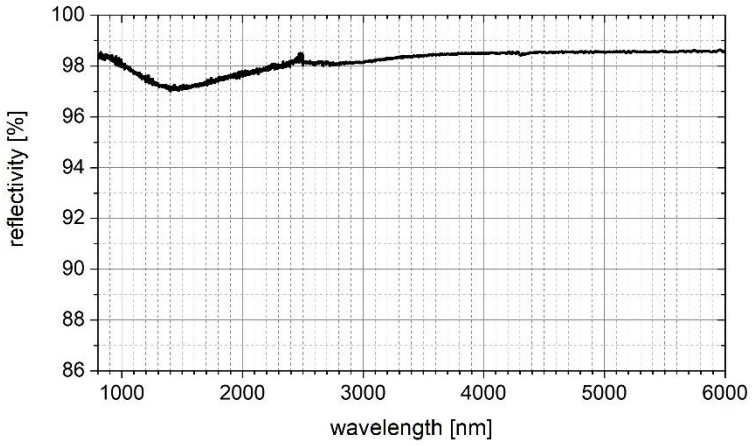

Figure 5: Optical performance of the protected Ag-coating applied for the IR spectrograph CRIRES$^+$ (measured at 6° AOI using a Lambda UV/VIS-spectrophotometer and Fourier Transform IR spectrometer from PerkinElmer).

REFERENCES

[1] Wilson, R. N., [Reflecting Telescope Optics II], Springer Berlin Heidelberg, Berlin, Heidelberg (2001).
[2] Thomas, N., Wolfe, J., "UV-Shifted Durable Silver Coating for Astronomical Mirrors," Proc. SPIE 4003, 312-323 (2000).
[3] Veleva, L., Valdez, B., Lopez, G. et al., "Atmospheric corrosion of electro-electronics metals in urban desert simulated indoor environment," Corrosion Engineering, Science and Technology 43 (2), 149-155 (2013).
[4] Vargas, O. L., Valdez, S. B., Veleva, M. L. et al. "The corrosion of silver in indoor conditions of an assembly process in the microelectronics industry," Anti-Corrosion Meth & Material 56 (4), 218-225 (2009).
[5] Jobst, P. J., Stenzel, O., Schürmann, M. et al., "Optical properties of unprotected and protected sputtered silver films: Surface morphology vs. UV/VIS reflectance," Advanced Optical Technologies 3 (1), 91-102 (2014).
[6] Thomas, N. L., Siekhaus, W. J., Farmer, J. C. et al., "Prevention of corrosion of silver reflectors for the National Ignition Facility," Proc. SPIE 3427, 394-400 (1998).
[7] Hass, G., Heaney, J. B., Herzig, H. et al., "Reflectance and durability of Ag mirrors coated with thin layers of Al_2O_3 plus reactively deposited silicon oxide," Applied optics 14 (11), 2639-2644 (1975).
[8] Pellicori, S. F., Scattering defects in silver mirror coatings," Appl. Opt. 19 (18), 3096-3098 (1980).
[9] Vucina, T., Boccas, M., Araya, C. et al. "Gemini primary mirror in situ wash," Proc. SPIE 7012, 1-13 (2008).
[10] Chu, C-T., Fuqua, P. D., Barrie, J. D. "Corrosion characterization of durable silver coatings by electrochemical impedance spectroscopy and accelerated environmental testing," Appl. Opt. 45 (7), 1583-1593 (2006).
[11] Folgner, K. A., Chu, C-T., Lingley, Z. R. et al. "Environmental durability of protected silver mirrors prepared by plasma beam sputtering," Appl. Opt. 56 (4), 75-86 (2017).
[12] Barrie, J. D., Fuqua, P. D., Folgner, K. A. et al. "Control of stress in protected silver mirrors prepared by plasma beam sputtering," Appl. Opt. 50 (9), 135-140 (2011).
[13] Schwinde, S., Schürmann, M., Jobst, P.J. et al. "Description of particle induced damage on protected silver coatings," Appl. Opt. 54, 4966-4971 (2015).

[14] Herrmanna, M., Schilma, J., Michaela, G. et al. "Corrosion of Silicon Nitride Materials in Acidic and Basic Solutions and under Hydrothermal Conditions," Journal of the European Ceramic Society 23, 585-594 (2003).
[15] Lin, C-H., Komeya, K., Meguro, T. et al. "Corrosion Resistance of Wear Resistant Silicon Nitride Ceramics in Various Aqueous Solutions," J. Ceram. Soc. Japan 111, 452-456 (2003).
[16] Vogel, W., [Glaschemie] Springer-Verlag Berlin, (1992).
[17] Salh, R. [Defect Related Luminescence in Silicon Dioxide Network: A Review], InTech-Verlag, (2011).
[18] Waters, P., Volinsky, A.A., "Stress and Moisture Effects on Thin Film Buckling Delamination," Experimental Mechanics 47, 163-170 (2007).
[19] Leplan, H., Geenen, B., Robic, J.Y. et al., "Residual stresses in evaporated silicon dioxide thin films: Correlation with deposition parameters and aging behavior" Journal of Applied Physics 78 (2), 962-968 (1995).
[20] Schwinde, S., Schürmann, M., Kaiser, N. et al., "Investigation of SiO_2-Al_2O_3 nanolaminates for protection of silver reflectors," Appl. Opt. 56, 41-46 (2017).
[21] Berg, S., Nyberg, T. "Fundamental understanding and modeling of reactive sputtering processes," Thin Solid Films 476, 215-230 (2005).
[22] Sheikh, D. A., Connell, S. J., Dummer, R. S. "Durable silver coating for Kepler Space Telescope primary mirror," Proc. SPIE 7010 1-5 (2008).
[23] Kinast, J., Schlegel, R., Kleinbauer, K., Steinkopf, R, Follert, R. et al. "Manufacturing of aluminum mirrors for cryogenic applications," Proc. SPIE 10706 (2018).
[24] Dorn, R. J., Anglada-Escude, G., Baade, D. al., "CRIRES+: Exploring the Cold Universe at High Spectral Resolution," The Messenger 156, 7-11 (2014).
[25] Berg, S., Larsson, T., Nender, C. et al. "Predicting thin-film stoichiometry in reactive sputtering," Journal of Applied Physics 63, 887-891 (1988).
[26] Särhammar, E., Strijckmans, K., Nyberg, T. et al. "A study of the process pressure influence in reactive sputtering aiming at hysteresis elimination," Surface and Coatings Technology 232, 357-361 (2013).
[27] OptiChar: Module of the software package OptiLayer for design and characterization of optical coatings (2013).
[28] Tencor FLX-2320 User Manual, "Thin Film Stress Measurement" (1995).
[29] Depla, D. [Magnetrons, reactive gases and sputtering], Ghent University Belgium, (2014).
[30] Huheey, J. E., Keiter, E. A., Keiter, R. L., [Anorganische Chemie: Prinzipien von Struktur und Reaktivität], de Gruyter, Berlin (2003).
[31] Cartledge, G. H., "Studies on the Periodic system – the ionic potential as a periodic function," 1. Journal of the American Chemical Society 50 (11), 2855-2863 (1928).
[32] Sree, K. S. [Principle of physical vapor deposition of thin films], Elsevier (2006).
[33] Blasek, G., Bräuer, G. [Vakuum Plasma Technologien: Beschichtung und Modifizierung von Oberflächen], Eugen G. Leutze Verlag (2010).
[34] Thornton, J. A., "Influence of substrate temperature and deposition rate on structure of thick sputtered Cu coatings," Journal of Vacuum Science and Technology 11, 666–670 (1974).
[35] Hirsch, E. H. "Stress in porous thin films through absorption of polar molecules," J. Phys. D: Appl. Phys. 13, 2081-2094 (1980).
[36] Stolz, C. J., Taylor, J. R., Eickelberg, W. K. et al. "Effects of vacuum exposure on stress and spectral shift of high reflective coatings," Appl. Opt., 32 (28), 5666–5672 (1993).
[37] Nishikawa, T., Ono, H., Murotani, H. et al. "Analysis of long-term internal stress and film structure of SiO_2 optical thin films," Appl. Opt. 50 (9), 210-216 (2011).
[38] Scherer K., Nouvelot, L., Lacan, P. et al. Optical and mechanical characterization of evaporated SiO_2 layers. Long-term evolution. Applied optics 35 (25): 5067-5072 (1996).
[39] Schulz, U., Jakobs, S., Norbert, K., "SiO_2 protective coatings on plastic optics deposited with plasma-lAD," Proc. SPIE 2776, 169-174 (1996).
[40] Bräuer, G., Szczyrbowski, J., Teschner, G. "Mid frequency sputtering - a novel tool for large area coating," Surface and Coatings Technology 94-95, 658–662 (1997).
[41] Besland, M-P., Lapeyrade, M., Delmotte, F. et al. "Interpretation of stress variation in silicon nitride films deposited by electron cyclotron resonance plasma," J. Vac. Sci. Technol A 22(5), 1962-1970 (2004).
[42] Schürmann, M., Schwinde, S., Kaiser, N., "Optical element comprising a reflective coating" EP3158370A1 (2017).